

Above-Threshold Ionization with Subpicosecond Laser Pulses

R. R. Freeman, P. H. Bucksbaum, H. Milchberg, S. Darack, D. Schumacher, and M. E. Geusic^(a)

AT&T Bell Laboratories, Murray Hill, New Jersey 07973

(Received 23 June 1987)

Above-threshold ionization (ATI) is investigated in xenon with pulses of light at 616 nm ranging from 15 to 0.4 psec. Significant energy shifts and broadenings of the ATI peaks are observed. For pulse widths less than 1 psec, the individual ATI peaks break up into a narrow fine structure, apparently due to resonance enhancements in the ionization process produced by ponderomotive shifts of states.

PACS numbers: 32.80.Rm

The name "above-threshold ionization" (ATI) is given to the process by which an atom in an intense optical field absorbs s more photons than the minimum number, n , necessary to reach the ionization limit, I_0 . In this process many peaks are observed in the photoelectron spectrum¹; and under the usual experimental conditions of a long laser pulse, the peaks are found to have relatively narrow widths, and energies given by

$$E = (n + s)\hbar\omega - I_0. \quad (1)$$

Recent experimental studies in the long-pulse regime have shown that the number² and intensity of peaks in the electron spectra,³ their angular distributions,⁴ and the peak widths⁵ all depend upon the intensity of the ionizing radiation; however, the recorded electron kinetic energies are nearly independent of intensity.⁶ This independence arises from the nearly complete cancellation of the increased ionization energy of the atom at the time of ionization and the kinetic energy gained by the electron from ponderomotive acceleration as it leaves the interaction volume.⁷

An ATI experiment is considered to be in the long-pulse regime if the duration of the ionizing radiation is long compared to the time it takes a photoelectron to leave the interaction volume. For typical electron energies and focal waists (2 eV, 20 μm), a laser pulse longer than 20 psec is in the long-pulse regime. Luk *et al.* have recently reported ATI results in the short-pulse regime using 248-nm radiation.⁸

In this Letter we present measurements of ATI in xenon using variable pulse widths of 616-nm light that pass from the long-pulse to the extreme short-pulse limit. Our results show how the short-pulse regime develops as a function of pulse width, and at pulse widths less than 1 psec, we have observed a remarkable new phenomenon: Each low-energy ATI peak breaks up into a series of narrow (instrument-limited) peaks.

An atom in an intense low-frequency radiation field experiences an ionization potential (I.P.) increase⁹ of

$$U_p = e^2 F_0^2 / 4m\omega^2, \quad (2)$$

where F_0 is the peak electric field of the optical wave at

the position of the atom. A photoelectron that would have kinetic energy $E = E_0$ in a weak field is instead produced in an intense field at kinetic energy $E = E_0 - U_p$. The ponderomotive energy of the newly created photoelectron in the optical field at the same location is also U_p . Thus for long pulses, the electron converts the ponderomotive energy into kinetic energy as it exits from the interaction volume, just compensating for the decrease in its initial kinetic energy due to the raised ionization potential. Because of this conservative nature of the ponderomotive potential, it has been virtually impossible to observe the effects of the I.P. shift on the energy spectra in long-pulse ATI experiments.¹⁰ The ponderomotive potential itself can be clearly discerned by its effect on the electron momenta.⁴

If the pulse duration of the ionizing radiation is short compared to the time for the photoionized electron to escape the interaction volume, there is no time for the photoelectron to accelerate before the pulse leaves. *In the limit of very short pulse duration, the electron energy spectrum records the actual photoelectron energies and angular distributions at the moment of ionization.*

Short pulses of linearly polarized laser light at approximately 616 nm were focused in xenon vapor by a 10-cm lens ($\approx f/20$) to nearly the diffraction-limited waist size (6 μm). The xenon gas density ($\approx 10^{10} \text{ cm}^{-3}$) was adjusted to ensure that space-charge effects were completely negligible. The photoelectrons for each laser pulse were recorded by means of a time-of-flight electron spectrometer and transient digitizer, and summed by a computer into separately stored spectra according to the laser energy for that pulse.

The light pulses were derived from a synchronously model-locked dye laser, amplified at 10 Hz to energies up to 1 mJ/pulse. Adjustable pulse widths between 5 and 20 psec were achieved by our varying the length of the dye-laser oscillator cavity; pulse lengths of 0.5–1.0 psec were derived by standard fiber-grating compression techniques.¹¹ The pulse widths were measured by autocorrelation in potassium dihydrogen phosphate.

Figure 1 shows the results of ATI measurements using ≈ 0.5 mJ/pulse. The photon energy was 2.01 eV; the

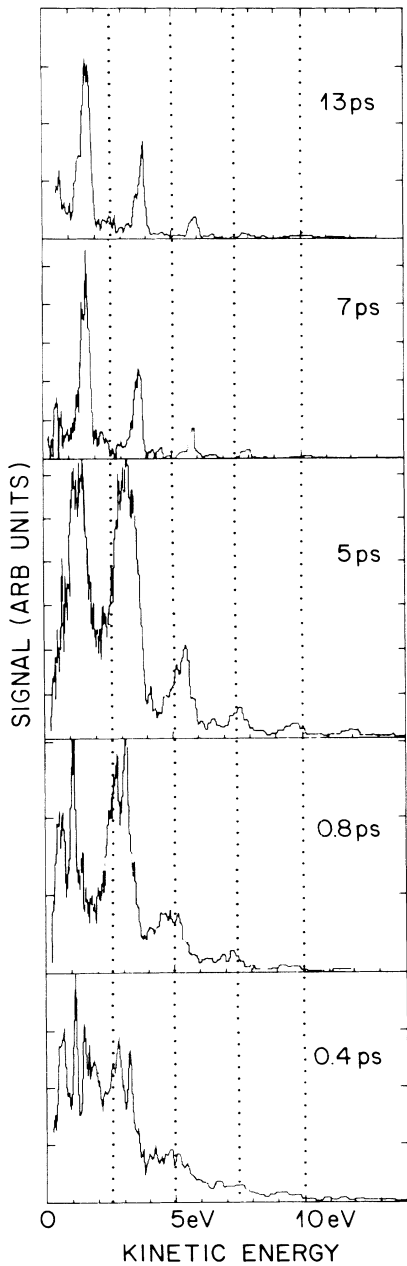


FIG. 1. Kinetic energy of photoelectrons emitted from xenon as a function of pulse width. The pulse energy is held roughly constant for all runs, so the intensity increases from $\approx 1.2 \times 10^{13}$ W/cm² for 15 psec to $\approx 3.9 \times 10^{14}$ W/cm² for 0.4 psec. For the shortest-pulse widths, the individual ATI peaks break up into a narrow fine structure.

peak intensity (ponderomotive potential) ranged from $\approx 1.2 \times 10^{13}$ W/cm² (0.45 eV) at 13 psec to $\approx 3.9 \times 10^{14}$ W/cm² (14.8 eV) at 0.4 psec. In the strictly long-pulse regime, the ATI peaks for the ²P_{3/2} core should appear near 2, 4, 6, 8, . . . , eV. At 13 psec the *s*=0 and 1 peaks are shifted to slightly lower energies, but the *s*=2

and higher are at their expected values. At 7 and 5 psec, the peaks show progressively more shift and broadening, and at less than 1 psec, the shift saturates.¹²

For pulse lengths shorter than 1 psec, each of the low-energy ATI peaks breaks up into a series of extremely narrow lines; the energies of the fine-structure lines were found to be independent of the laser intensity, the spatial mode, or focusing. Each fine-structure peak in *s*=0 is repeated 2.01 eV ($\hbar\omega$) higher in energy in *s*=1 and is even found in *s*=2, although the resolution is degraded above 4 eV.

To analyze our data we have employed a time-dependent generalization of ponderomotive scattering. The *time-dependent* force that a free electron feels at position **r**, for a pulse with intensity *I*(**r**,*t*) [$=F_0(\mathbf{r},t)^2/8\pi c$], is $= -\nabla[e^2 F_0(\mathbf{r},t)^2/4m\omega^2]$. The intensity distribution in the focus is assumed to be Gaussian:

$$I(r, z, t) = [r_0^2 P_0 / r(z)^2] e^{-[r/r(z)]^2} e^{-[(t-z/c)/(\tau/2)]^2},$$

where $r(z)^2 = r_0^2 [1 + (\lambda z / \pi r_0^2)^2]$, τ is the pulse length, r_0 is the spot size at the waist, and P_0 is the peak intensity at $r=z=t=0$.

The initial direction of the electrons is along the polarization,⁴ and the initial energies are shifted for each electron as a result of the local ionization-potential shift of the atom at the time of ionization. The probability of *n*th-order ionization, P^n , at (*r*,*z*,*t*) is taken as

$$P^n(r, z, t) = [I(r, z, t) / I_0]^n \exp \left\{ - \int_{-\infty}^t [I(r, z, t') / I_0]^n dt' \right\}.$$

I_0 is related to the experimental "saturation intensity," above which the integrated ionization probability at the focus goes to 1. At the shortest pulse widths, the energy shift is equal to the shift in the ionization potential at the moment of ionization. Because most of the electrons ionize at or near the saturation intensity, the *average* shift of an ATI peak roughly determines the saturation intensity through the relation $1 \text{ eV} = 2.6 \times 10^{13} \text{ W/cm}^2$ for light at 616 nm. From Fig. 1, the saturation value for our data is approximately 1.2 eV, or $3.1 \times 10^{13} \text{ W/cm}^2$.

Figure 2 shows the results of the full space-time computer simulation for an *s*=2 ATI peak using our focusing parameters. As the pulse width narrows, the peaks broaden and shift, reproducing our data from the long- to the short-pulse regime.¹³ The success of this simulation is consistent with and supports the central role of the ponderomotive potential in ATI, from the increase in the ionization potential of neutral atoms to the determination of the final energy of the photoionized electrons.

Ponderomotive energy shifts are evidently also responsible for the fine structure observed within each ATI grouping for pulse widths less than 1 psec: Weakly

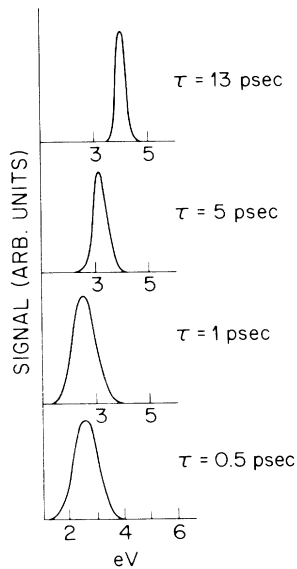


FIG. 2. Results of the space-time simulation described in the text for an $s=2$ ATI peak with weak-field kinetic energy of 4 eV.

bound excited states of xenon all shift upward along with the ionization potential by approximately U_p . These levels will therefore come into resonance with a harmonic of the laser field at some intensity, resulting in a resonant enhancement in the ionization rate. Since the electron's kinetic energy is tied to the intensity according to Eq. (2), the energy spectrum records a peak for each occurrence of resonance enhancement. The position of the peak is independent of the temporal and spatial inhomogeneity of the laser pulse. If the shift of a state with an original energy E_i above the ground state is U_p , it will produce a peak in the spectrum at energy

$$E = (n+s)\hbar\omega - I_0 - (m\hbar\omega - E_i), \quad (3)$$

where the intermediate resonant enhancement occurs for m ($=6$, here) photons. Thus, the fine structure in the electron energy spectrum is predicted to be the direct result of resonance enhancements.

The potential six-photon resonant enhancements in xenon involve even-parity intermediate states $5p^5(^2P_{3/2})nl$, for $l=p, f, h, \dots$. Figure 3 records the positions of each state of this type listed by Moore¹⁴ and mapped according to Eq. (3) onto our data for the $s=1$ ATI group. We stress that there are *no* adjustable parameters. With the exception of the missing peak corresponding to the $5p^5(^2P_{3/2})10p$ state, the agreement of the positions of the tabulated levels and the experimental peaks for energies greater than 0.8 eV is surprisingly good. Indeed, we did not expect states as deeply bound as the $7p$ or the $4f$ to have their shifts given so nearly by U_p . The residual mismatch between tabulated levels and experimental

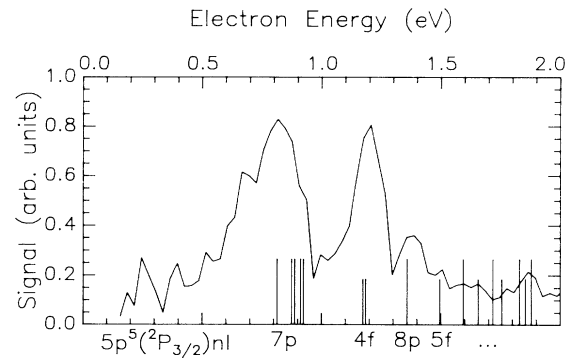


FIG. 3. $s=0$ fine-structure data for pulse widths less than 0.5 psec; also plotted is the location, according to Eq. (3), of the relevant $5p^5(^2P_{3/2})nl$ states from Moore (Ref. 14). The instrument resolution, which increases as the square root of the energy, is 0.05 eV at 0.5 eV and 0.1 eV at 2.0 eV. With the exception of the missing peak corresponding to the $5p^5(^2P_{3/2})10p$ (1.72 eV) state, the experimental spectrum is reasonably well assigned above 0.8 eV. As discussed in the text, the peaks in the spectrum below 0.8 eV may have their origin in the blend of a large number of states, including $m=5$ odd-parity resonances.

peaks most likely is due to additional ac Stark shifts of the levels not given by Eq. (3).

We have not attempted to assign the spectrum in the region below 0.8 eV, because unlike the higher-energy region, there are too many possible energy levels of xenon which could contribute. These include $m=5$, $5p^5(^2P_{3/2})6s$ odd-parity resonances, as well as an entire series of $5p5ns'[\frac{1}{2}]_1$, $5p5nd'[\frac{3}{2}]_1$, and $5p5nd'[\frac{5}{2}]_{2,3}$ autoionizing resonances between the $P_{1/2}$ and $P_{3/2}$ limits. These latter states contribute resonances¹⁵ from $m=7$ at energies between 0.3 and 0.8 eV.

The intensities of the resonant enhancements depend on several factors: the total volume experiencing a given intensity; the relative oscillator strengths; and most importantly, the highly nonlinear ionization rate as a function of intensity. This last factor probably accounts for the large enhancements for the $7p$ and $4f$ states, because these states require greater intensities to be shifted into the $m=6$ resonance than do higher-lying ones, and thus have a relatively larger ionization rate at resonance.

Finally, we note that the fine structure will appear only for the shortest-pulse excitations. For longer pulses, all the electrons will leave the interaction volume during the pulse and arrive at the detector with the *same* weak-field value of kinetic energy.

The results of this work strongly suggest that the excited states of the atom *do* play a crucial role in determining the properties of ATI, even when the experiment is nominally "nonresonant." For example, the angular distribution of electrons *within* each ATI group may be strongly influenced by the transient resonant enhance-

ments they experience at the moment of ionization. We conclude that the use of ultrashort-pulse excitation in high-intensity multiphoton ionization experiments provides a means of obtaining spectroscopic data on target atomic or molecular species without the masking effects of final-state (ponderomotive) scattering.

We wish to acknowledge helpful discussions with W. E. Cooke, T. J. McIlrath, and A. Szoke.

^(a)Current address: Battelle Northwest Laboratories, Richland, WA 99352.

¹P. Agostini, F. Fabre, G. Mainfray, G. Petite, and N. Rahman, *Phys. Rev. Lett.* **42**, 1127 (1979); P. Kruit, J. Kimman, and M. van der Wiel, *J. Phys. B* **14**, L597 (1981); G. Petite, F. Fabre, P. Agostini, M. Crance, and M. Aymar, *Phys. Rev. A* **29**, 2677 (1984).

²P. Kruit, J. Kimman, and M. van der Wiel, *Phys. Rev. A* **28**, 248 (1983); L. A. Lompre, A. L. Huillier, G. Mainfray, and C. Manus, *J. Opt. Soc. Am. B* **2**, 1906 (1985).

³Kruit, Kimman, and van der Wiel, Ref. 1; L. A. Lompre, G. Mainfray, C. Manus, and J. Thebault, *Phys. Rev. A* **15**, 1604 (1977); P. H. Bucksbaum, M. Bashkansky, R. R. Freeman, T. J. McIlrath, and L. DiMauro, *Phys. Rev. Lett.* **56**, 2590 (1986); G. Petite, P. Agostini, and F. Yergeau, *J. Opt. Soc. Am. B* **4**, 765 (1987).

⁴R. R. Freeman, T. J. McIlrath, P. H. Bucksbaum, and M. Bashkansky, *Phys. Rev. Lett.* **57**, 3156 (1986).

⁵Petite, Agostini, and Yergeau, Ref. 3; P. H. Bucksbaum, R. R. Freeman, M. Bashkansky, and T. J. McIlrath, *J. Opt.*

Soc. Am. B **4**, 760 (1987); T. J. McIlrath, P. H. Bucksbaum, R. R. Freeman, and M. Bashkansky, *Phys. Rev. A* **35**, 4611 (1987).

⁶Kruit, Kimman, and van der Wiel, Ref. 1; Lompre *et al.*, Ref. 2; Bucksbaum *et al.*, Ref. 5.

⁷M. Mittleman, *J. Phys. B* **17**, L351 (1984); E. Fiordilino and M. Mittleman, *J. Phys. B* **18**, 4425 (1985); M. J. Hollis, *Opt. Commun.* **25**, 395 (1978).

⁸T. S. Luk, T. Graber, H. Jara, U. Johann, K. Boyer, and C. K. Rhodes, *J. Opt. Soc. Am. B* **4**, 847 (1987).

⁹Bucksbaum *et al.*, Ref. 5; Mittleman, Ref. 7.

¹⁰Petite, Agostini, and Yergeau (Ref. 3) have demonstrated resolved energy shifts in ATI peaks in the intermediate-pulse-width regime using 50-psec Nd-doped yttrium-aluminum-garnet laser pulses; see also P. Agostini, J. Kupersztych, L. A. Lompre, G. Petite, and F. Yergeau, *Phys. Rev. A* (to be published).

¹¹W. J. Tomlinson, R. H. Stolen, and C. V. Shank, *J. Opt. Soc. Am. B* **1**, 139 (1984).

¹²The saturation of the energy shift and its insensitivity to intensity for the shortest pulses is in agreement with the results reported for 248-nm excitation by Luk *et al.*, Ref. 8.

¹³This simulation used a Gaussian pulse in both space and time; however, the essential results were found to be unaltered when pulses with rather significant distortions in both space and time were used.

¹⁴C. E. Moore, *Atomic Energy Levels*, U. S. National Bureau of Standards Circular No. 467 (U.S. GPO, Washington, DC, 1949).

¹⁵K. Yoshino and D. E. Freeman, *J. Opt. Soc. Am. B* **2**, 1268 (1985).